A compact frequency selective stop-band splitter by using Fabry–Perot nanocavity in a T-shaped waveguide*

M Afshari Bavil and Sun Xiu-Dong(孙秀冬)†

Department of Physics, Harbin Institute of Technology, Harbin 150001, *China*

(Received 2 July 2012; revised manuscript received 4 August 2012)

By utilizing a Fabry–Perot (FP) nanocavity adjacent to T-shaped gap waveguide ports, spectrally selective filtering is realized. When the wavelength of incident light corresponds to the resonance wavelength of the FP nanocavity, the surface plasmons are captured inside the nanocavity, and light is highly reflected from this port. The resonance wavelength is determined by using Fabry–Perot resonance condition for the nanocavity. For any desired filtering frequency the dimension of the nanocavity can be tailored. The numerical results are based on the two-dimensional finite difference time domain simulation under a perfectly matched layer absorbing boundary condition. The analytical and simulation results indicate that the proposed structure can be utilized for filtering and splitting applications.

Keywords: T-shaped splitter, Fabry–Perot nanocavity, spectrally selective splitting, finite difference time domain (FDTD) simulation

PACS: 78.68.+m, 68.47.De, 42.79.Fm **DOI:** 10.1088/1674-1056/22/4/047808

1. Introduction

Surface plasmon polaritons (SPPs) are a special kind of electromagnetic field, which are confined in the interface between metal and dielectric. SPPs propagate along the interface with an exponentially decaying field in both sides.[1] The most interesting property of SPPs is that they are not constrained by optical diffraction limit.[2] Therefore, SPPs are considered as one of the most promising ways for overcoming the diffraction limit at subwavelength scale.[3] Recently, many plasmonic devices for light control were theoretically and/or experimentally demonstrated.[4–9] Because of the strong localization, low bend loss and easier fabrication procedure, metal–dielectric–metal (MDM) configuration has attracted much attention. To date, several novel plasmonic waveguides-based MDM structures such as U-shaped,[10] T-shaped splitters,[11] and Y-shaped combiners and splitters have been proposed.[12]

A light splitter, which can divide light into several channels, is a vital component for nanophotonic integrated circuits.[11,12] The simplest splitter is a T-shaped splitter, which identically splits light power in the whole frequency range through the ports. Proportional power splitting through the desired ports has been reported by changing the ports width.[13,14] Otherwise, an SPP ring resonator and SPP coupler structure have realized the spectrally selective light splitting numerically and experimentally in Refs. [13] and [14]. However, finding a compact structure for spectrally selective splitting has been quite a challenge. Qi *et al.*[11] proposed a T-shaped splitter with engraved periodic grooves inside the port as a frequency splitter, which for desired frequencies the period, width, and thickness of the grooves can be adjusted. Gong *et al.*[13] numerically demonstrated that spectral splitting could be obtained by drilling nanocavities at each port. The dimensions of the nanocavities can be tailored to tune the desired splitting through the ports. Despite the aforementioned structure, realizing more functional and practical splitters each with a lower loss, higher transmissivity and compact dimension is still under study.

In this paper, a new kind of compact T-shaped MDM splitter with embedded Fabry–Perot cavity adjacent to the output port is proposed and analyzed. For the resonance wavelength of the cavity, light can be reflected from the port. The resonance wavelength is calculated by using the FP resonance condition for the nanocavity. The physics behind this filtering is explained by using the FP resonator and effective refractive index concept. The spectral filtering can be achieved for any desired frequency by tuning the effective refractive index. The finite-difference time-domain (FDTD) simulation with a perfectly matched layer (PML) absorbing boundary condition is employed as a numerical tool. Due to its compact dimension and simple configuration, this device can be utilized in nanophotonic integrated circuits.

2. Structure and theoretical analysis

The point is how to control the SPPs propagating through the splitter. In order to make the generated SPPs travel or stop along the ports, we place a nanocavity next to the port. First, the case of a nanocavity close to the left port is considered. Figure 1 shows the schematic of the proposed structure. w, w_1, h, and g denote the slit width, nanocavity width, nanocavity length, and the coupling distance between port and nanocavity, respectively.

* Project supported by the National Key Basic Research Program of China (Grant No. 2013CB328702).

† Corresponding author. E-mail: xdsun@hit.edu.cn

© 2013 Chinese Physical Society and IOP Publishing Ltd

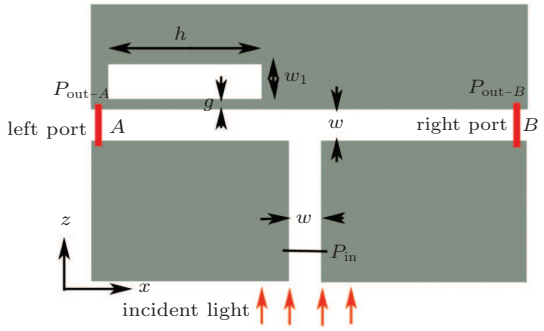


Fig. 1. (color online) Schematic plot of the designed structure. The input, output ports, and nanocavity have identical widths of $w = w_1 =$ 50 nm, the light is p-polarized and impinges from the bottom. The nanocavity thickness, $h = 500$ nm, the distance between the nanocavity and left port g is 20 nm. A, B are monitors to detect the transmission fields.

It is clear to see from Fig. 1 that a metallic layer with a slit makes a metal–dielectric–metal waveguide. Surface plasmon polaritons (SPPs) are excited at the metal/dielectric (MD) interface by p-polarized incident light. The only surface plasmon polariton mode surviving for all values of the slit is called gap surface plasmon polariton (TM_0 mode). The complex propagation constant β of TM_0 mode can be obtained by solving the dispersion relation.[15] The effective refractive index of the metal–dielectric–metal waveguide can be expressed as $N_{\text{eff}} = \beta/k_0$, where k_0 is the vacuum wave vector. The dependence of the effective refractive index on slit width is given by the following equation[15]

$$\mathrm{N_{eff}} \approx \sqrt{\varepsilon_{\mathrm{d}} + 0.5\left(\frac{k^0_{\mathrm{gap}}}{k_0}\right)^2 + \sqrt{\left(\frac{k^0_{\mathrm{gap}}}{k_0}\right)^2\left(\varepsilon_{\mathrm{d}} - \varepsilon_m + 0.25\left(\frac{k^0_{\mathrm{gap}}}{k_0}\right)^2\right)}}, \quad k^0_{\mathrm{gap}} = -\frac{2\varepsilon_{\mathrm{d}}}{w\varepsilon_m}, \tag{1}$$

where w is the slit width, ε_{m} and ε_{d} are the permittivities of the metal and dielectric, respectively. The dielectric in the slit, nanocavity and surrounding media are assumed to be all in vacuum state ($\varepsilon_{\mathrm{d}} = 1$). The structure is considered as a silver, of which the permittivity is characterized by the Drude model

$$\varepsilon_{\mathrm{m}}(\omega) = \varepsilon_\infty - \frac{\omega_{\mathrm{p}}^2}{\omega^2 + \mathrm{i}\omega\gamma}, \tag{2}$$

where $\omega_{\mathrm{p}} = 1.34 \times 10^{16}$ Hz and $\gamma = 2.12 \times 10^{14}$ Hz, ω_{p} and γ are the bulk plasma frequency and damping frequency of the oscillations respectively, ω is the angular frequency of the incident electromagnetic radiation, and ε_∞ is the high-frequency bulk permittivity with a value of 4.1.[16] The effective refractive index for the cavity can also be obtained from Eq. (1). The dependence of the refractive index on the slit or cavity parameters provides a way of controlling the SP propagation. The real part of N_{eff} provides phase retardation, which is an important parameter for structure based on a Fabry–Perot resonator. Figure 2 shows the relationship between the real part of N_{eff}, slit or cavity width and wavelength. N_{eff} may be slightly varied by changing the wavelength; however it strongly depends on slit or cavity width. The effective refractive index decreases by increasing the slit or cavity width. The imaginary part is given by $\alpha = 4\pi/\lambda_0 \mathrm{Im}(N_{\text{eff}})$, which represents the propagation loss coefficient. In the case of our study, we are only concerned with the real part of N_{eff}.

When the incident optical wave travels along the port, parts of the wave are coupled into the nanocavity. A stable standing wave can only build up constructively within the "cavity" when the resonant condition is satisfied. Based on the principle of a resonant cavity, the resonant condition can be determined by the following equation:

$$2\frac{2\pi}{\lambda_{\mathrm{m}}}\mathrm{Re}(N_{\text{eff}})h + \Delta\phi = 2m\pi, \tag{3}$$

where h is the length of the nanocavity, N_{eff} is the effective refractive index of coupled-SPPs (waveguide mode) inside the nanocavity, and $\Delta\phi$ is an additional phase shift experienced by the fundamental mode. Positive integer m is the number of antinodes of the standing SPP wave. The resonant wavelengths of the nanocavity can be obtained by rearranging Eq. (3) as

$$\lambda_{\mathrm{m}} = \frac{2\mathrm{Re}(N_{\text{eff}})h}{m - \Delta\phi/2\pi}. \tag{4}$$

It can be seen from Eq. (4) that the resonance wavelengths are all proportional to the length of the "resonant cavity" (h), and the effective refractive index (N_{eff}) is related to nanocavity width (w_1) via Eq. (1) and phase shift $\Delta\phi$. In Eq. (4) the term of $\Delta\phi/2\pi$ is very small. Moreover, the effective index of the nanocavity segment also depends on the coupling strength with the port. Therefore there is a relation between the effective index and the gap between the cavity and port, and the resonant wavelength is dependent on the gap in some way.

First, second and higher resonance orders can be easily obtained by inserting $m = 1$, $m = 2$, and other higher order quantities in Eq. (4). At the resonance wavelength, the nanocavity resonance mode will be excited and the nanocavity will trap the SPPs passing through the port. As a result, the light propagation will be blocked through the port and light will transmit solely through the remote port. This is a mechanism of a spectral light splitter. The resonance wavelength can be adjusted to desired wavelengths by changing the nanocavity

parameters and coupling distance. The desired spectral plasmonics splitter can be determined by proper geometrical parameters such as length, width of the nanocavity, and coupling distance.

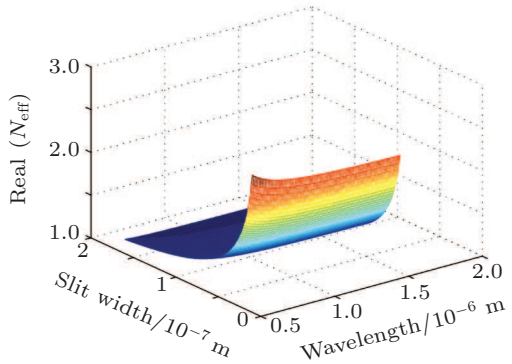


Fig. 2. (color online) Dependence of real part of the effective refractive index on slit width and incident wavelength.

3. Numerical results

To reveal the validity of the theoretical predictions, the numerical tools using two-dimensional (2D) FDTD simulation is employed to study the optical behavior of the structure. In the simulation, the spatial mesh steps are set to be $\Delta x = \Delta z = 4$ nm in order to keep the convergence, and the time step is $\Delta t = \Delta x/2c$ (c is the velocity of light in the vacuum). The calculated region is truncated by using perfectly matched layer absorbing boundary conditions on the boundaries. To obtain a transmission profile, a normally incident p-polarized plane wave, whose magnetic field component is parallel to the slit (along the y direction), with a wavelength of 632.8 nm impinging from the bottom is employed. The widths of power monitors, as shown on Fig. 1, are set to be wider than the port widths at points A and B to detect the electromagnetic fields. The incident power $P_{\rm in}$ and the transmitted power $P_{\rm out}$ are calculated by integrating the normal component of the time-averaged Poynting vector of $\boldsymbol{S}_{\rm avg}=\frac{1}{2}\,{\rm Re}\,(\boldsymbol{E}\times\boldsymbol{H}^{*})$ where $\boldsymbol{E}$ and $\boldsymbol{H}$ denote the electric and magnetic fields, respectively. The transmission ratio is defined as $T = P_{\rm out}/P_{\rm in}$. In the T-shaped splitter, the light propagating through the bottom channel is equally divided into two beams and they enter into the left and right ports, respectively. However, the insertion of a nanocavity affects the light propagation and imposes stop-band nature at the specific wavelengths. First, we consider a single cavity and the geometrical parameters are set to be $w_1 = 50$ nm, $h = 500$ nm, $w = 50$ nm, and $g = 20$ nm. For brevity, only the second order resonance mode is considered in this work. From Eq. (4), the second order FP resonance mode is located around 790 nm. Figure 3 shows the transmission spectrum of the structure with the wavelength-selective characteristic of a typical filter. The minimum transmittance occurs at a wavelength of 800 nm, which corresponds to the second order resonance peak of the nanocavity. The third order resonance mode can be seen on the transmission spectrum as well. It is obvious from the transmission spectrum that the transmission through the left port approaches to zero when the resonance wavelength of the cavity is excited.

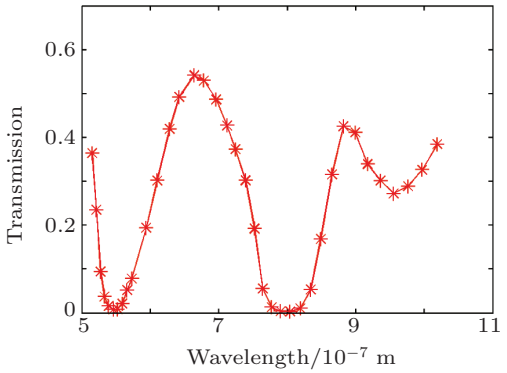


Fig. 3. (color online) Transmission profile of the left port as a function of wavelength. The minimum transmissions appear at 800 nm and 546 nm which correspond to second and third order resonance peaks, respectively.

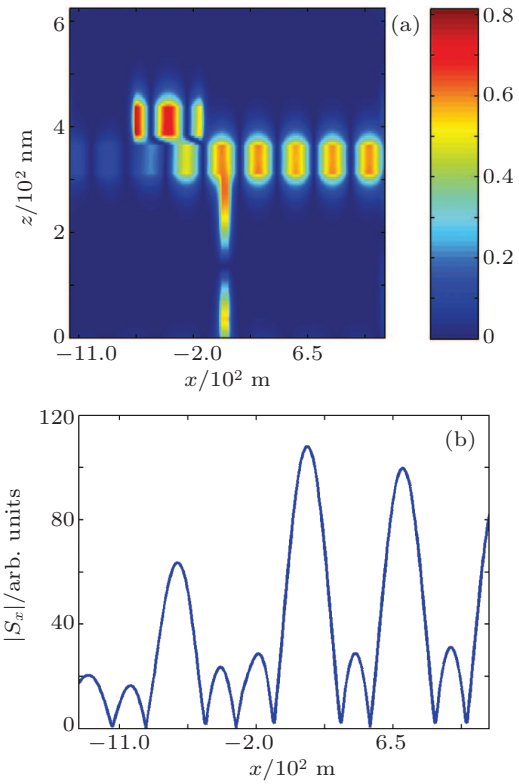


Fig. 4. (color online) (a) Distribution of magnetic field $|H_y|$. The wavelength of incident light is 800 nm; at this wavelength the nanocavity stops SPPs propagating through the left port. (b) The Poynting field along the x direction in the middle of the output port.

The distributions of magnetic field $|H_y|$ and Poynting field $|S_x|$ are shown in Fig. 4. When the wavelength of incident light corresponds to cavity resonance mode, the cavity resonance mode is excited and captures the SPs propagating through the left port as predicted. The simulation result in Fig. 4(a) displays that the light is reflected from the left port and merely

is guided through the right port. Figure 4(b) reveals the x-component of the Poynting field $|S_x|$ along the x direction in the middle of the output channel. It is obvious that the main portion of the energy is transferred through the right port, however, the Poynting field amplitude decays along the left port due to absorption loss.

The coupling distance between the nanocavity and port, g, should be investigated in depth. To estimate this distance, some considerations on the coupling distance should be performed. The penetration depth of the SPPs in the metal is given by

$$\delta_{\mathrm{m}} = \frac{1}{k_0}\left|\frac{\varepsilon'_{\mathrm{m}}+\varepsilon_{\mathrm{d}}}{\varepsilon'^2_{\mathrm{m}}}\right|^{1/2},$$

where $\varepsilon'_{\mathrm{m}}$ represents the real part of the metal permittivity.[17] The penetration depth differs slightly from the wavelength in our working wavelength range. The penetration depth is approximately 30 nm for our structure. The taking of a value smaller than 30 nm for the gap between port and nanocavity provides the coupling between nanocavity and port. For this reason, the gap between the nanocavity and port (g) is taken to be 20 nm to insure the coupling. Our simulation also reveals that for much smaller values of g the nanocavity and the port couple strongly and weaken the "cavity" effect, which reduces the output power. Due to the coupling effect, the nanocavity should be located far from the output interface to prevent tunnelling effect.

Figure 5(a) shows the transmission spectra of the structure at different gaps, while the nanocavity width and length are set to be 50 nm and 500 nm, respectively. Figure 5(b) shows the second ($m = 2$) and third ($m = 3$) order resonance wavelength dependence on the coupling distance. The resonance wavelengths shift slightly toward a shorter wavelength with gap increasing and the bandwidths become a bit narrower at the same time. The phenomenon of gap-dependence of resonance wavelength can be attributed to the weak dependence of the effective index on the gap. This is because N_{eff} of the region is different from that of the standard MDM waveguide. The larger the coupling distance, the less the deviation from the standard MIM waveguide is and the smaller the N_{eff} is. Moreover, the bandwidths of minimum points in transmission profile become a bit narrower with g increasing, because a large coupling distance results in a small coupling strength, which will enhance the "cavity" effect due to the small amount of energy coupled out of the nanocavity. Furthermore, by increasing the gap, the transmission of resonance wavelength is far from zero, owing to the fact that light trapping efficiency of the cavity decreases with gap increasing.

Afterwards, the nanocavities with different widths adjacent to both ports are introduced to obtain a splitter with spectrally selective function in both directions as shown in Fig. 6(a). Due to effective refractive index dependence on nanocavity parameters, various nanocavities result in different resonance modes. Therefore, any desired splitting frequency can be obtained by utilizing various nanocavities. Here, the widths of left and right nanocavity are considered to be 80 nm and 40 nm, respectively. The lengths of the nanocavities are both set to be 500 nm. The widths of input and output ports are kept the same as the previous ones.

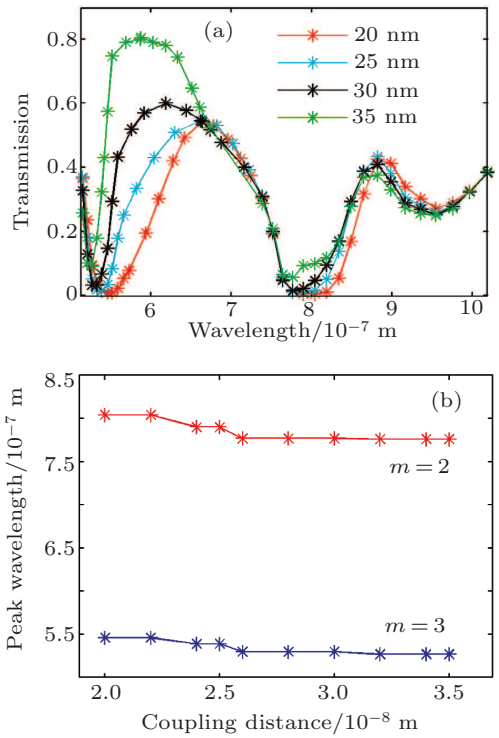


Fig. 5. (color online) (a) Transmission spectra of the structure for different coupling distances, and (b) dependences of second and third peak wavelengths on coupling distance.

Figure 6(b) shows the transmission spectra of the structure as a function of wavelength. The minimum transmittances in the transmission profiles of left and right ports correspond to nanocavities? resonance modes. Attention is paid to the second order resonances for brevity. The explanation can be easily generalized to other resonance orders. The second order resonances for left and right nanocavities occur at 710 nm and 840 nm, respectively. Third order resonance mode can also be seen in the transmission spectra. Figure 7 shows the distributions of magnetic field $|H_y|$ and Poynting field at the resonance wavelength 710 nm. As seen from Fig. 7(a), at this wavelength the resonance mode of the left nanocavity is excited and captures the SPPs. Therefore, the light transmission is blocked through this port. However, light is guided through the right port. The light intensity in the left port decays along the port as shown in Fig. 7(b), which confirms the light is captured within the cavity. Furthermore, the light intensity passing through the right port is small compared with that in the non-cavity case, which can be attributed to the loss effect in the presence of the nanocavity.

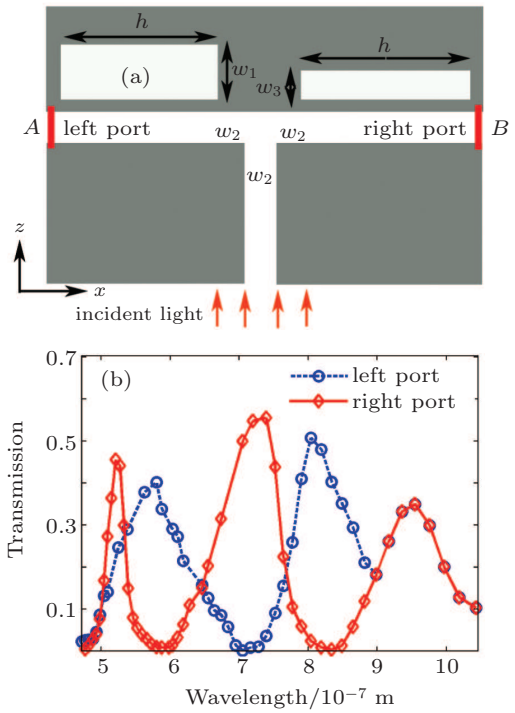


Fig. 6. (color online) (a) Schematic plot of spectrally selective splitter. The nanocavity lengths are both set to be 500 nm, and $w_1 = 80$ nm and $w_2 = 40$ nm. The coupling distances between the nanocavity and port are all 20 nm. (b) Transmission profile of the structure as a function of wavelength. The minimum transmission points correspond to the resonance modes of nanocavities. The circle and square curves are the outputs of left and right ports, respectively.

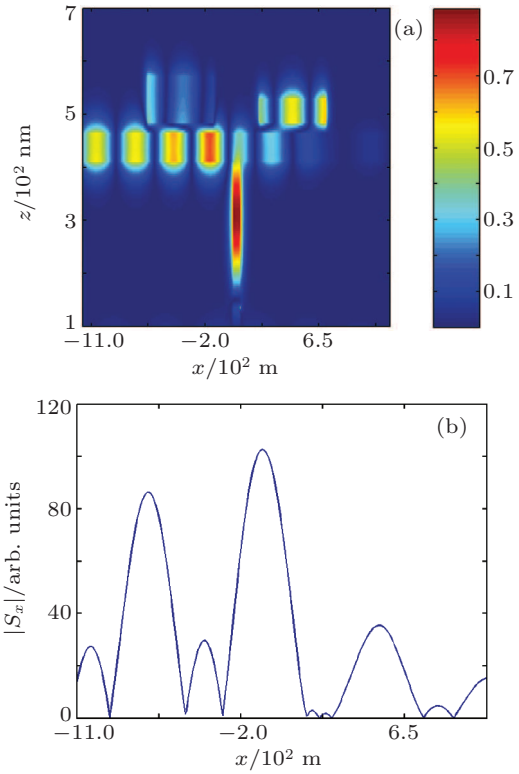


Fig. 8. (color online) (a) magnetic field $|H_y|$ distribution when the wavelength of incident light is 840 nm. At this wavelength, the right nanocavity stops SPPs propagating through the right port, and (b) the Poynting field along the x direction in the middle of the output port.

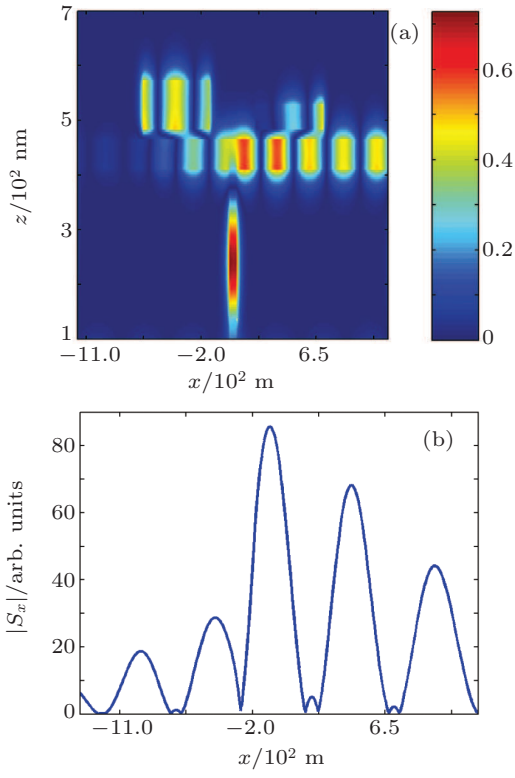


Fig. 7. (color online) (a) Magnetic field $|H_y|$ distribution when the wavelength of the incident light is 710 nm. At this wavelength, the left nanocavity stops SPPs propagating through the left port, and (b) Poynting field along the x direction in the middle of the output port.

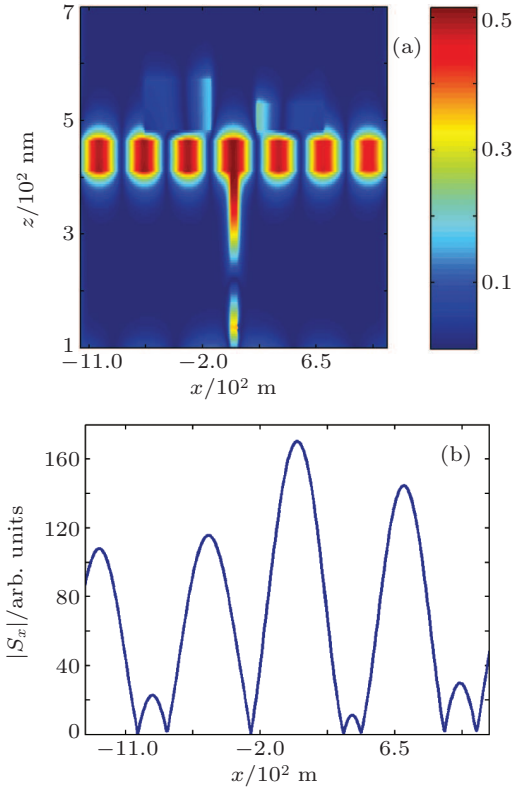


Fig. 9. (color online) (a) Distribution of magnetic field $|H_y|$. The wavelength of incident light is 950 nm; for this wavelength, the nanocavities do not affect SPPs travelling through the ports; (b) The Poynting field along the x direction in the middle of the output port.

Figure 8 shows the simulation result for the incident light with a wavelength of 840 nm. As seen from Fig. 8(a), at this wavelength, the resonance mode of the right nanocavity is excited and traps the SPPs; therefore, the light can be guided only through the left port. The light intensity in the right port is decaying as shown in Fig. 8(b), which means that the light transmission is blocked through the right port.

For the rest of the wavelengths, the nanocavities do not affect the splitting nature, each of which behaves as a regular T-shaped splitter. The simulation result for one of the non-resonance frequencies is shown in Fig. 9. The light beams transmitting through the ports in the presence and the absence of nanocavities are approximately identical. The small difference in throughput between the ports is due to the loss occurring in the presence of nanocavities.

As mentioned before, for the wavelengths satisfying the resonance conditions of the nanocavities via Eq. (4), the nanocavities stop the light transmission, which enables us to have a spectrally selective control of light transmission. It is shown that the resonance wavelengths depend on effective refractive index of the nanocavity, which is directly related to the nanocavity parameters.

4. Conclusions

In this paper, an approach based on a Fabry–Perot resonator nanocavity for spectral splitting is suggested. The light is captured within the cavity when the wavelength of incident light satisfies the nanocavity resonance condition. For the rest of the wavelength spectra, the presence of nanocavities does not affect the light transmission nature. By using the FP resonance condition of the nanocavity, the resonance wavelengths are determined. Obviously, one can realize the function of selecting any wavelength in the way of changing the parameters of the nanocavity, such as width, length, and coupling distance. We believe that this compact and simple structure will facilitate the design of nanoscale structures, which can be utilized in integrated optical circuits and opto-electronic applications such as SPP transistors.

References

[1] Raether H 1988 *Surface Plasmon on Smooth and Rough Surfaces and on Gratings* (Berlin: Springer-Verlag) p. 5
[2] Barnnes W L, Dereux A and Ebbesen T W 2003 *Nature* **424** 824
[3] Ozbay E 2006 *Science* **311** 189
[4] Baida F I, Belkhir A, Labeke D V and Lamrous O 2006 *Phys. Rev. B* **74** 205419
[5] Houseini A, Nejati H and Massoud Y 2008 *Opt. Express* **16** 1475
[6] Verhagen E, Polman A and Kuipers L 2008 *Opt. Express* **16** 45
[7] Lee H S, Yoon Y T, Lee S S, Kim S H and Lee K D 2007 *Opt. Express* **15** 15457
[8] Xue W R, Guo Y N and Zhang W M 2010 *Chin. Phys. B* **19** 017302
[9] Li X F, Pan S, Guo Y N and Wang Q 2011 *Chin. Phys. B* **20** 015204
[10] Lee T and Gray S 2005 *Opt. Express* **13** 9652
[11] Qi Y, Gan D, Ma J, Cui J, Wang C and Luo X 2009 *Appl. Phys. B* **95** 807
[12] Gao H T, Shi H F, Wang C T, Du C L, Luo X G, Deng Q L, Lü Y G, Lin X D and Yao H M 2005 *Opt. Express* **13** 10795
[13] Gong Y K, Liu X M, Wang L R and Zhang Y N 2011 *Opt. Commun.* **284** 795
[14] He M D, Liu J Q, Gong Z Q, Luo Y F, Chen X S and Lu W 2010 *Opt. Commun.* **283** 1784
[15] Bozhevolnyi S 2009 *Plasmonic Nanoguides and Circuits* (Singapore: Pan Stanford Publishing Pte. Ltd.) p. 200
[16] Shuford K L, Ratner M A, Gray S K and Schatz G C 2006 *Appl. Phys. B* **84** 11
[17] Barnes W L 2006 *J. Opt. A: Pure Appl. Opt.* **8** S87